

**Observational constraints on modified gravity models and the Poincaré dodecahedral topology**M. C. Bento,<sup>1,\*</sup> O. Bertolami,<sup>1,†</sup> M. J. Rebouças,<sup>2,‡</sup> and N. M. C. Santos<sup>3,§</sup><sup>1</sup>*Departamento de Física, Instituto Superior Técnico, Avenida Rovisco Pais, 1049-001 Lisboa, Portugal*<sup>2</sup>*Centro Brasileiro de Pesquisas Físicas Rua Dr. Xavier Sigaud 150 22290-180 Rio de Janeiro -RJ, Brazil*<sup>3</sup>*Institut für Theoretische Physik, Universität Heidelberg Philosophenweg 16, 69120 Heidelberg, Germany*

(Received 3 April 2006; published 31 May 2006)

We study observational constraints on models that account for the accelerated expansion of the universe via infrared modifications to general relativity, namely, the Dvali-Gabadadze-Porrati braneworld model as well as the Dvali-Turner and Cardassian models. We find that significant constraints can be placed on the parameters of each model using type Ia supernovae data together with the baryon acoustic peak in the large-scale correlation function of the Sloan Digital Sky Survey of luminous red galaxies and the Cosmic Microwave Background Radiation shift parameter data. Moreover, by considering the Poincaré dodecahedral space as the circles-in-the-sky observable spatial topology, we show that the detection of a such a nontrivial topology would provide relevant additional constraints, particularly on the curvature parameter, for all models.

DOI: [10.1103/PhysRevD.73.103521](https://doi.org/10.1103/PhysRevD.73.103521)

PACS numbers: 98.80.-k, 95.36.+x, 98.80.Es, 98.80.Jk

**I. INTRODUCTION**

Models where gravity is modified by soft very long-range corrections, normally inspired in braneworld constructions, are an interesting approach to account for the recent accelerated expansion of the universe, with no need for dark energy. One of the simplest covariant modified-gravity models is based on the Dvali-Gabadadze-Porrati (DGP) braneworld model [1], as generalized to cosmology by Deffayet [2]. In this model, gravity is altered at large distances by the slow leakage of gravity off our 4-dimensional brane universe into the 5-dimensional bulk space time, leading to a modification of the Friedmann equation in a cosmological context. At small scales, gravity becomes effectively bound to the brane and 4D gravity is recovered to a good approximation. Crucially for our purposes, it was shown by Deffayet that the model exhibits cosmological solutions with a self-accelerating phase at late times. An interesting variation of this proposal has been suggested by Dvali and Turner [3] (hereafter referred to as DT model). Another possibility, also originally motivated by extra dimensions physics, is the modification of the Friedmann equation by the introduction of an additional nonlinear term proportional to  $\rho^n$ , the so-called Cardassian model [4].<sup>1</sup>

We analyze current constraints on the parameters of these models, as provided by the so-called *gold* sample of 157 type Ia supernovae (SNe Ia) [6], as well as the

baryon oscillation acoustic peak (BAO) in the large-scale correlation function of the Sloan Digital Sky Survey (SDSS) [7] and the cosmic microwave background radiation (CMBR) shift parameter [8]. We consider a nonflat prior. Notice that joint SNe-CMBR-BAO constraints have already been considered for the  $\Lambda$ CDM and quintessence models in Ref. [9] and for an f(R) modified-gravity model in [10]. While this work was in progress, the corresponding analysis for the DGP model has appeared, see Ref. [11], where the authors conclude that both flat DGP and  $\Lambda$ CDM models are within the 1 sigma contour, but the latter provides a better fit to the data. In what concerns the DT and Cardassian models, constraints from supernovae data alone have previously been studied, see [12] and references therein.

Likewise for dark energy models, one expects the parameters of modified-gravity models to be affected by the geometry of the universe. The description of the universe as a metrical manifold, requires the characterization of its geometry and its topology; hence, a key issue regarding our understanding of the universe concerns its 3-dimensional geometry and topology. Studies of the CMBR such as the ones performed by the Wilkinson Microwave Anisotropy Probe (WMAP) allow for testing geometry, which is related with the intrinsic curvature of the 3-dimensional space. On the other hand, topology concerns global properties of space such as its shape and size and, clearly, 3-geometry restricts but does not determine the topology of its spatial section. However, in a locally spatially homogeneous and isotropic universe, the topology of its spatial sections determines the sign of its local curvature [13] and therefore dictates its geometry.

Different strategies and methodologies have been devised to probe a putative nontrivial topology of the spatial sections of the universe (see, e.g. Refs. [14,15] for reviews and details on cosmic crystallographic methods). For in-

\*Electronic address: bento@sirius.ist.utl.pt; Also at Centro de Física Teórica de Partículas, Instituto Superior Técnico, Avenida Rovisco Pais, 1049-001 Lisboa

†Electronic address: orfeu@cosmos.ist.utl.pt

‡Electronic address: reboucas@cbpf.br

§Electronic address: n.santos@thphys.uni-heidelberg.de

<sup>1</sup>Other braneworld models could also be considered, e.g. the model proposed in Ref. [5].

stance, the so-called circles-in-the-sky method, is based on the presence of multiple images of correlated circles in the CMBR maps [16]. In a space with a detectable nontrivial topology, the last scattering sphere (LSS) intersects some of its topological images along pairs of circles of equal radii, centered at different points on the LSS, with the same distribution of temperature fluctuations,  $\delta T$ . These pairs of matching circles will be imprinted on the CMBR anisotropy sky maps regardless of the background geometry or detectable topology [16,17]. Hence, it follows that in order to probe observationally a nontrivial topology, one should examine the full-sky CMBR maps in order to extract the correlated circles, and use their angular radii and the relative position of their centers to probe a putative nontrivial topology of the spatial sections of the observable universe.

In particular, it has been shown that the Poincaré dodecahedral space topology (see Section IVA) accounts for the low value of the CMBR quadrupole and octopole moments measured by first year WMAP data [18], which has been confirmed by the most recent WMAP data analysis [19], and fits the temperature two-point correlation function [20–22]. Recently, the Poincaré dodecahedral space [22], through the circles-in-the-sky method, has been considered as the observable spatial topology of the universe in order to reanalyze the current SNe Ia plus X-ray gas mass fraction constraints on the density parameters of matter ( $\Omega_m$ ) and dark energy ( $\Omega_\Lambda$ ) in the context of the  $\Lambda$ CDM model [23], with the result that it considerably reduces degeneracies. The circles-in-the-sky method has also been used to place constraints on the parameters of the generalized Chaplygin gas (GCG) model [24–26], as discussed in Ref. [27]. In that work, by using both the Poincaré dodecahedral and binary octahedral topologies, it has been shown that these spatial topologies through circles-in-the-sky could provide additional constraints on the  $A_s$  parameter of the GCG model as allowed by the SNe Ia observations.

Given these encouraging results it is natural to use this strategy to constrain the parameters of modified-gravity models as well. To this end, we will consider the Poincaré dodecahedral space topology to reanalyze current constraints on the parameters of the DGP, DT and Cardassian models, in a joint analysis with the observational constraints mentioned above, namely, the *gold* sample of SNe Ia, as well as the baryon oscillation acoustic peak in the large-scale correlation function of the SDSS and the CMBR shift parameter.

## II. MODIFIED-GRAVITY MODELS

Modified-gravity models explore the possibility that there is no dark energy, and consider instead that infrared modifications to general relativity exist on very large scales, accounting in this way for the observed late time acceleration of the universe.

### A. Dvali-Gabadadze-Porrati model

One of the simplest covariant modified-gravity models is based on the DGP braneworld model [1], as generalized in Ref. [2] to a FLRW brane in a Minkowski bulk.

In the DGP model, standard model gauge fields are confined to a (3 + 1)D brane residing in an noncompact (4 + 1)D bulk, with different scales of gravity on the brane and in the bulk. The gravitational part of the action is given by

$$S = \frac{M_5^3}{2} \int d^4x dw \sqrt{g^{(5)}} R_5 + \frac{M_{\text{Pl}}^2}{2} \int d^4x \sqrt{g} R_4, \quad (1)$$

where  $M_5$  denotes the 5D Planck mass,  $M_{\text{Pl}}$  is the 4D Planck mass,  $g^{(5)}$  is the trace of the 5D metric  $g_{AB}^{(5)}$  ( $A, B = 0, 1, 2, \dots, 4$ ),  $w$  is the extra spatial coordinate,  $g$  the trace of the 4D metric induced in the brane,  $g_{\mu\nu}(x) \equiv g_{\mu\nu}^{(5)}(x, w = 0)$ , and where  $R_5, R_4$  are the 5D and 4D scalar curvatures, respectively. This gravitational action coupled to matter on the brane leads to a modified Friedmann equation, which can be written as [2]

$$H^2 + \frac{k}{a^2} = \left( \sqrt{\frac{8\pi\rho}{3M_{\text{Pl}}^2} + \frac{1}{4r_c^2}} + \frac{1}{2r_c} \right)^2, \quad (2)$$

where

$$r_c = \frac{M_{\text{Pl}}^2}{2M_5^3} \quad (3)$$

is a length scale beyond which gravity starts to leak out into the bulk.

Rewriting the above equation in dimensionless variables  $\Omega_x = \rho_x/\rho_{\text{crit}}$  with  $\rho_{\text{crit}} = 3M_{\text{Pl}}^2 H_0^2/8\pi$  and  $\rho_x$  the energy density in the component  $x$  today, we get

$$\left( \frac{H}{H_0} \right)^2 = \Omega_k (1+z)^2 + \left( \sqrt{\Omega_m (1+z)^3 + \Omega_{r_c}} + \sqrt{\Omega_{r_c}} \right)^2, \quad (4)$$

where  $H_0$  is the Hubble expansion parameter today and  $z$  is the redshift, and we have taken into account that, at present, the universe is matter dominated, hence  $\rho \simeq \rho_m$ . Moreover,  $\Omega_k = -k/(a_0^2 H_0^2)$  is the present curvature parameter and

$$\sqrt{\Omega_{r_c}} = \frac{1}{2r_c H_0}. \quad (5)$$

The constraint equation between the various components of energy density at  $z = 0$  is then given by

$$\Omega_k + \left( \sqrt{\Omega_{r_c} + \Omega_m} + \sqrt{\Omega_{r_c}} \right)^2 = 1. \quad (6)$$

It has been shown that the observed recent acceleration of the universe can be obtained from the extra contribution to the Friedmann equation by setting the length scale  $r_c$  close to the horizon size [28,29].

### B. Dvali-Turner model

Inspired in the above construction, Dvali and Turner considered a more generic modification of the Friedmann equation [3], hereafter referred to as DT model

$$H^2 + \frac{k}{a^2} = \frac{8\pi\rho}{3M_{\text{Pl}}^2} + \frac{1}{r_c^{2-\beta}} \left( H^2 + \frac{k}{a^2} \right)^{\beta/2}. \quad (7)$$

Notice that  $\beta$  is the only parameter of the model: the case  $\beta = 1$  corresponds to the DGP model,  $\beta = 0$  to the cosmological constant case, and  $\beta = 2$  to a ‘‘renormalization’’ of the Friedmann equation. A stringent bound follows from requiring that the new term does not interfere with the formation of large-scale structure,  $\beta \leq 1$ , whereas the successful predictions of Big Bang nucleosynthesis impose a weaker limit on  $\beta$ , namely,  $\beta \leq 1.95$ . Moreover, it can be shown that this correction behaves like dark energy in the recent past, with equation of state  $w_{\text{eff}} = -1 + \beta/2$ , and  $w = -1$  in the distant future; moreover, it can mimic  $w < -1$  without violating the weak-energy condition [3].

The expression for the Hubble expansion as a function of redshift is then

$$\begin{aligned} \left( \frac{H}{H_0} \right)^2 - 2\sqrt{\Omega_{r_c}} \left[ \left( \frac{H}{H_0} \right)^2 - \Omega_k(1+z)^2 \right]^{\beta/2} \\ = \Omega_m(1+z)^3 + \Omega_k(1+z)^2, \end{aligned} \quad (8)$$

where  $\Omega_{r_c}$  is now generalized to

$$\sqrt{\Omega_{r_c}} = \frac{1}{2(r_c H_0)^{2-\beta}}, \quad (9)$$

which means that the constraint between the various densities at  $z = 0$  is given by

$$\Omega_m + \Omega_k + 2\sqrt{\Omega_{r_c}}(1 - \Omega_k)^{\beta/2} = 1. \quad (10)$$

### C. Cardassian model

We will also consider the so-called Cardassian model [4], which explains the current acceleration of the universe by a modification of the Friedmann equation consisting basically in the introduction of an additional term proportional to  $\rho^n$

$$H^2 = \frac{8\pi}{3M_{\text{Pl}}^2} (\rho + b\rho^n) - \frac{k}{a^2}, \quad (11)$$

where  $b$  and  $n$  are constants, and we have added a curvature term to the original Cardassian model. As in the previous cases, in this model the universe is composed only of radiation and matter (including baryon and cold dark matter) and the energy density required to close the universe is much smaller than in standard cosmology, so that matter can be sufficient to provide a flat (or close to flat) geometry.

For  $n < 1$  the second term becomes important if  $z < \mathcal{O}(1)$ ; thereon it dominates the Friedmann equation and yields  $a \propto t^{2/3n}$  for ordinary matter, so acceleration will occur if  $n < 2/3$ . There are two main motivations for the introduction of the extra term, namely, terms of that form typically when the universe is embedded as a three-dimensional surface (3-brane) in higher dimensions [30] or, alternatively, it may appear in a purely 4D theory due to an extra contribution to the total energy density as would be the case if there were some unknown interactions between matter particles [31].

In a matter dominated universe, Eq. (11) can be rewritten as

$$\begin{aligned} \left( \frac{H}{H_0} \right)^2 = \Omega_m(1+z)^3 + \Omega_k(1+z)^2 \\ + (1 - \Omega_m - \Omega_k)(1+z)^{3n}. \end{aligned} \quad (12)$$

Notice that the case  $n = 0$  corresponds to the  $\Lambda$ CDM model.

Finally, it is worth pointing out that these models have been thoroughly scrutinized from the observational point of view using constraints from CMBR, SNe Ia and large scale structure. For recent studies see, for instance, Refs. [11,12,32–39].

## III. OBSERVATIONAL CONSTRAINTS

### A. Constraints from SNe Ia

For our analysis, we consider the set of SNe Ia data recently compiled by Riess *et al.* [6] known as the *gold* sample. This set contains 157 points: 143 points taken from the 230 Tonry *et al.* [40] data plus 23 points from Barris *et al.* [41] and 14 points discovered using HST [6]. Various points where the classification of the supernovae was uncertain or the photometry was incomplete have been discarded, thus increasing the reliability of the sample. The data points in the *gold* sample are given in terms of the distance modulus

$$\mu_{\text{obs}}(z) \equiv m(z) - M_{\text{obs}}(z), \quad (13)$$

and the respective errors  $\sigma_{\mu_{\text{obs}}}(z)$ , which already take into account the effects of peculiar motions. The apparent magnitude  $m$  is related to the dimensionless luminosity distance

$$D_L(z) = \frac{1+z}{\sqrt{|\Omega_k|}} S(y(z)), \quad (14)$$

where  $S(x) \equiv (\sin(x), \sinh(x), x)$  for  $\Omega_k < 0$ ,  $\Omega_k > 0$  and  $\Omega_k = 0$ , respectively, by

$$m(z) = \mathcal{M} + 5\log_{10} D_L(z). \quad (15)$$

We have defined a new function

$$y(z) \equiv \sqrt{|\Omega_k|} \int_0^z \frac{H_0}{H(z')} dz'.$$

The  $\chi^2$  is calculated from

$$\chi_{\text{SN}}^2 = \sum_{i=1}^n \left[ \frac{\mu_{\text{obs}}(z_i) - \mathcal{M}' - 5 \log_{10} D_{\text{Lth}}(z_i; \alpha_i)}{\sigma_{\mu_{\text{obs}}}(z_i)} \right]^2, \quad (16)$$

where  $\mathcal{M}' = \mathcal{M} - M_{\text{obs}}$  is a nuisance parameter,  $\alpha_i$  are the model parameters and  $D_{\text{Lth}}(z; \alpha_i)$  is the theoretical prediction for the dimensionless luminosity distance determined using the modified Friedmann equations.

### B. Constraints from the SDSS baryon acoustic oscillations

In order to further remove degeneracies intrinsic to the distance fitting methods, it is interesting to consider also the effect of the baryon acoustic peak of the large scale correlation function at  $100h^{-1}$  Mpc separation, detected by the SDSS team using a sample of LRG [7]. The position of the acoustic peak is related to the quantity

$$\mathcal{A} = \sqrt{\Omega_m} \left( \frac{H_0}{H(z_{\text{lr}})} \right)^{1/3} \left[ \frac{1}{z_{\text{lr}} \sqrt{|\Omega_k|}} S(y(z_{\text{lr}})) \right]^{2/3}, \quad (17)$$

which takes the value  $\mathcal{A}_0 = 0.469 \pm 0.017$ , and where  $z_{\text{lr}} = 0.35$  [7]. We have neglected the weak dependence of  $\mathcal{A}_0$  on the spectral tilt. The baryon acoustic peak is taken into account by adding the term

$$\chi_{\text{sdss}}^2 = \left( \frac{\mathcal{A}_0 - \mathcal{A}}{\sigma_{\mathcal{A}}} \right)^2 \quad (18)$$

to the  $\chi^2$ , where  $\sigma_{\mathcal{A}}$  is the error of  $\mathcal{A}_0$ .

We should point out that there is a level of uncertainty in the measurement of  $\mathcal{A}$  due to uncertainties essentially on  $\Omega_m$  (notice that uncertainties on the baryon density  $\Omega_b$  are constrained by the CMBR and Big Bang nucleosynthesis to be smaller than about 2%). Also, one should notice that the baryon acoustic oscillations were analyzed using a fiducial  $\Lambda$ CDM model and the full data set was compressed to a constraint at a single redshift [7]. As pointed out by Dick *et al* [42], the reduction of the data was intended to be valid for the case of a  $\Lambda$ CDM model and robust for models with a constant equation of state, but may give rise to significant systematic errors for the models we are considering. Although a reanalysis of the baryon oscillation data in the context of these models would no doubt be desirable, one may argue that substantial changes are not to be expected given that the modifications of gravity we are considering are supposed to alter general relativity only at the Gpc scale. The same can be said about topology given that it affects only the low modes of the CMBR spectrum.

### C. Constraints from the CMBR shift parameter

It is expected that when the cosmological parameters are varied, there is a shift in the whole CMBR angular spectrum, that is  $\ell \rightarrow \mathcal{R}\ell$ , with the shift parameter  $\mathcal{R}$  being given by [8]

$$\mathcal{R} = \sqrt{\frac{\Omega_m}{|\Omega_k|}} S(y(z_{\text{ISS}})), \quad (19)$$

where  $z_{\text{ISS}} = 1089$  [18]. The results from CMBR (WMAP, CBI, ACBAR) data correspond to  $\mathcal{R}_0 = 1.716 \pm 0.062$  (using results from Spergel *et al.* [18]). We include the CMBR data in our analysis by adding

$$\chi_{\text{cmb}}^2 = \left( \frac{\mathcal{R}_0 - \mathcal{R}}{\sigma_{\mathcal{R}}} \right)^2, \quad (20)$$

to the total  $\chi^2$  function, where  $\mathcal{R}$  is computed for each model using Eq. (19).

## IV. COSMIC TOPOLOGY IN BRANE COSMOLOGY

In the framework of standard Friedmann-Lemaître-Robertson-Walker (FLRW) cosmology, the universe is described by a space-time manifold  $\mathcal{M}_4$  which is decomposed into  $\mathcal{M}_4 = \mathbb{R} \times M_3$  and endowed with a locally (spatially) homogeneous and isotropic metric

$$ds^2 = -dt^2 + a^2(t) \left[ \frac{dr^2}{1 - kr^2} + r^2(d\theta^2 + \sin^2\theta d\phi^2) \right], \quad (21)$$

where, depending on the sign of the constant spatial curvature  $k$ , the geometry of the 3-space  $M_3$  is either Euclidean ( $k = 0$ ), spherical ( $k = 1$ ), or hyperbolic ( $k = -1$ ).

Thus, since our 3-dimensional space  $M_3$  is chosen to be one of the following simply-connected spaces, Euclidean  $\mathbb{R}^3$ , spherical  $\mathbb{S}^3$ , or hyperbolic space  $\mathbb{H}^3$ , depending on the sign of the constant spatial curvature  $k$ , it is a common misconception that the Gaussian curvature  $k$  of  $M_3$  is all one needs to establish whether the 3-space where we live in is finite or not. However, it is known that the great majority of constant curvature 3-spaces,  $M_3$ , are multiply-connected quotient manifolds of the form  $\mathbb{R}^3/\Gamma$ ,  $\mathbb{S}^3/\Gamma$ , and  $\mathbb{H}^3/\Gamma$ , where  $\Gamma$  is a fixed-point free group of isometries of the corresponding covering space. Thus, for example, for the Euclidean geometry besides  $\mathbb{R}^3$  there are 6 classes of topologically distinct compact and orientable spaces  $M_3$  that can be endowed with this geometry, while for both the spherical and hyperbolic geometries there is an infinite number of nonhomeomorphic (topologically inequivalent) manifolds with nontrivial topology that admit these geometries. On the other hand, since the ultimate spatial topology has not yet been determined by cosmological observations, our 3-dimensional space may be any of these possible quotient manifolds.

Quotient manifolds are compact in three independent directions, or compact in two or at least one independent direction. In compact manifolds, any two given points may be joined by more than one geodesic. Since the radiation emitted by cosmic sources follows geodesics, the immediate observational consequence of a nontrivial detectable

spatial nontrivial topology<sup>2</sup> of  $M_3$  is that there will be multiple images of either cosmic objects or specific spots on the CMBR. At very large scales, the existence of these multiple images (or pattern repetitions) is a physical effect that can be used to probe the 3-space topology.

In 5D braneworld models, the universe is described by a 5-dimensional metrical orbifold (bulk)  $\mathcal{O}_5$  that is mirror symmetric ( $\mathbb{Z}_2$ ) across the 4D brane (manifold)  $\mathcal{M}_4$ . Thus, the bulk can be decomposed as  $\mathcal{O}_5 = \mathcal{M}_4 \times E_1 = \mathbb{R} \times M_3 \times \mathbb{E}_1$ , where  $E_1$  is a  $\mathbb{Z}_2$  symmetric Euclidean space, and where  $\mathcal{M}_4$  is endowed with a Robertson-Walker metric Eq. (21), which is recovered when  $w = 0$  for the extra noncompact dimension. In this way, the multiplicity of possible inequivalent topologies of our 3-dimensional space, and the physical consequences of a nontrivial detectable topology of  $M_3$  (possible multiple images of discrete cosmic sources, circle-in-the-sky on the LSS) is brought on the braneworld scenario.

### A. Poincaré dodecahedral space topology

The Poincaré dodecahedral space  $\mathcal{D}$  is a 3-manifold of the form  $\mathbb{S}^3/\Gamma$  in which  $\Gamma = I^*$  is the binary icosahedral group of order 120. It is represented by a regular spherical dodecahedron (12 pentagonal faces) along with the identification of the opposite faces after a twist of  $36^\circ$ . Such a space is positively curved ( $k = 1$ ,  $\Omega_k < 0$ ), and tiles the 3-sphere  $\mathbb{S}^3$  into 120 identical spherical dodecahedra.

The observed values of the power measured by WMAP of the CMBR quadrupole ( $\ell = 2$ ) and octopole ( $\ell = 3$ ) moments, and the sign of the curvature density  $\Omega_k = -0.02 \pm 0.02$  reported by first year WMAP data analysis team [18], which has been reinforced by the three-year WMAP observations (cf. Table 11 of Ref. [19]), have motivated the suggestion of the Poincaré dodecahedral space topology as an explanation for this observed large-angle anomaly in the CMB power spectrum [22]. This observation has sparked the interest in the dodecahedral space, which has been examined on its various features [20,21,44–46]. In particular, it turns out that a universe with the Poincaré dodecahedral space section accounts for the suppression of power at large angle observed by WMAP [18,19], and fits the WMAP temperature two-point correlation function [20,21], retaining the standard FLRW background for local physics. Notice however that a preliminary search of the antipodal matched circles in the WMAP sky maps predicted by the Poincaré model has failed [44]. A second search of the correlated circles for the  $\mathcal{D}$  space was not conclusive either [47]. This absence of evidence of correlated circles may be due to several causes, such as the Sunyaev-Zeldovich effect, lensing and the finite thickness of the LSS, as well as possible systematics in the removal of the foregrounds, which can damage the topo-

<sup>2</sup>The extent to which a nontrivial topology may be detected was discussed in Refs. [43].

logical circle matching. Thus, it is conceivable that the correlated circles may have been overlooked in the CMBR sky maps search [20].

Regarding the compatibility of the Poincaré dodecahedral space topology with string theory, it has been shown that, on account of the Adams-Polchinski-Silverstein conjecture on the instability of nonsupersymmetric AdS orbifold, the Poincaré dodecahedral space topology cannot arise as a model for the spatial sections of accelerating braneworld cosmological models in the framework of string theory [48]. However, while the braneworld paradigm has often been referred to as string-inspired, the models we are considering are not committed to that premise.

### B. The circles-in-the-sky method

An important class of constant curvature positively-curved 3-spaces with a nontrivial topology is comprised by the *globally homogeneous* manifolds. These manifolds satisfy the topological principle of (global) homogeneity, in the sense that all points in  $M_3$  are topologically equivalent. In particular, in these spaces the pairs of matching circles will be antipodal, as shown in Fig. 1.

The Poincaré dodecahedral space  $\mathcal{D}$  is globally homogeneous, and give rise to six pairs of antipodal matched circles on the LSS, centered in a symmetrical pattern as the centers of the faces of the dodecahedron. Figure 1 shows a pair of these antipodal circles. Clearly the distance between the centers of each pair of these correlated circles is twice the radius  $r_{\text{inj}}$  of the sphere inscribed in  $\mathcal{D}$ .

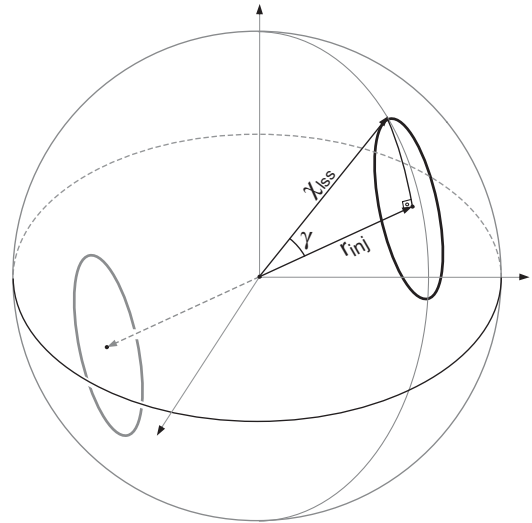


FIG. 1. A schematic illustration of two antipodal matching circles in the LSS. These pair of circles come about in all globally homogeneous positively-curved manifolds with a circles-in-the-sky detectable topology. The relation between the angular radius  $\gamma$ , angular sides  $r_{\text{inj}}$  and  $\chi_{1\text{ss}}$  is given by the following Napier's rule for spherical triangles,  $\cos \gamma = \tan r_{\text{inj}} \cot \chi_{1\text{ss}}$ .

It then follows from the use of trigonometric relations (known as Napier's rules) for the right-angled spherical triangle shown in Fig. 1 gives origin to a relation between the angular radius  $\gamma$ , the angular sides  $r_{\text{inj}}$  and radius  $\chi_{\text{lss}}$  of the LSS, namely

$$\chi_{\text{lss}} = \tan^{-1} \left[ \frac{\tan r_{\text{inj}}}{\cos \gamma} \right], \quad (22)$$

where  $r_{\text{inj}}$  is a topological invariant, equal to  $\pi/10$  for the space  $\mathcal{D}$ , and the distance  $\chi_{\text{lss}}$  to the origin is given by

$$\chi_{\text{lss}} = y(z_{\text{lss}}), \quad (23)$$

Equation (23) makes apparent that  $\chi_{\text{lss}}$  depends on the cosmological scenario. Moreover, Eq. (22) with  $\chi_{\text{lss}}$  given by Eq. (23) together with the ratio  $H_0/H$  for each modified-gravity model yield a relation between the angular radius  $\gamma$  and the cosmological parameters of each model. Thus, they can be used to set bounds (confidence regions) on model parameters. To quantify this, we consider a typical angular radius  $\gamma = 50^\circ$  estimated in Ref. [20] for the Poincaré dodecahedral space and, since the measurements of the radius  $\gamma$  do involve observational uncertainties on the model parameters from the detection of the spatial topology, we take into account these uncertainties; in order to obtain conservative results, we consider  $\delta\gamma \simeq 6^\circ$ , which is the scale below which the circles are blurred for the Poincaré dodecahedral space case [20].

### C. Constraints from cosmic topology

The effect of cosmic topology is taken into account by adding a new term to the  $\chi^2$  as

$$\chi_{\text{top}}^2 = \left( \frac{\chi_{\text{lss}} - \chi_{\text{lss}}^{\text{th}}}{\sigma_{\chi_{\text{lss}}}} \right)^2. \quad (24)$$

The value of  $\chi_{\text{lss}}$  is given by Eq. (23) and the uncertainty  $\sigma_{\chi_{\text{lss}}}$  comes from the uncertainty  $\delta\gamma$  of the circles-in-the-sky method. The theoretical value of  $\chi_{\text{lss}}$  for each model is obtained from  $\chi_{\text{lss}} = y(z_{\text{lss}})$  combined with the respective expansion law.

## V. RESULTS

We have performed a best-fit analysis with the minimization of the total  $\chi^2$ ,

$$\chi^2 = \chi_{\text{SN}}^2 + \chi_{\text{sdss}}^2 + \chi_{\text{cmb}}^2 + \chi_{\text{top}}^2, \quad (25)$$

for the modified-gravity models mentioned above using a MINUIT [49] based code. Notice that we marginalize analytically over  $\mathcal{M}'$  and that we allow the parameters  $\beta$  and  $n$  to vary in the interval  $]-10, 1]$  and  $]-10, 2/3[$ , respectively. In the cases where topology is taken into account, we use the prior  $\Omega_k < 0$  since the Poincaré dodecahedral space is positively curved. Our results are summarized in Table I.

In Fig. 2, we show the 1, 2 and 3 $\sigma$  confidence contours in the  $\Omega_m - \Omega_k$  plane for the  $\Lambda$ CDM and DGP models obtained using the SNe Ia gold sample, SDSS acoustic peak and CMBR shift parameter data (dashed lines). We also show the contours obtained assuming a  $\mathcal{D}$  space topology with  $\gamma = 50^\circ \pm 6^\circ$  (full lines). This figure together with Table I shows that the best-fit DGP model is slightly open whereas the best-fit  $\Lambda$ CDM model is slightly closed. Notice also that the effect of the CMBR shift parameter is to push the best-fit values for  $\Omega_k$  towards a flat universe, as first pointed out in Ref. [11], while the

TABLE I. Best-fit parameters for the  $\Lambda$ CDM, DGP, DT and Cardassian models for different combinations of observational constraints (SN = SNe Ia gold sample, BAO = SDSS baryon acoustic oscillations, CMBR = CMBR shift parameter and T = Poincaré dodecahedral space topology for  $\gamma = 50^\circ \pm 6^\circ$ ).

Model	Parameters	SN	SN + BAO	SN + BAO + CMBR	SN + BAO + CMBR + T
$\Lambda$ CDM	$\Omega_m$	0.46	0.28	0.28	0.29
	$\Omega_k$	-0.44	0.033	-0.003	-0.020
	$\chi^2$	181.24	183.76	183.93	184.44
DGP	$\Omega_m$	0.33	0.27	0.27	0.28
	$\Omega_k$	-0.56	-0.32	0.014	-0.021
	$\chi^2$	181.36	182.04	190.53	192.34
DT	$\beta$	-10	1.0	0.26	0.23
	$\Omega_m$	0.49	0.27	0.28	0.29
	$\Omega_k$	0.032	-0.32	-0.002	-0.02
	$\chi^2$	180.55	182.04	183.54	184.11
Card	$n$	-6.15	0.33	0.042	0.041
	$\Omega_m$	0.33	0.27	0.28	0.29
	$\Omega_k$	0.33	-0.76	-0.003	-0.020
	$\chi^2$	178.77	182.08	183.72	184.23

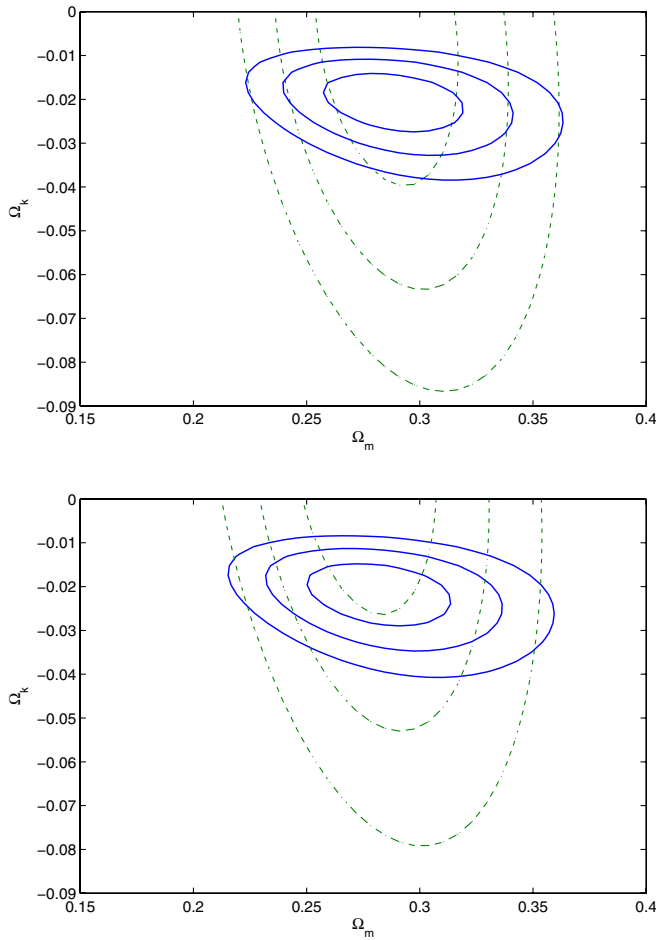


FIG. 2 (color online). Confidence contours (68.3%, 95.4% and 99.7%) in the  $\Omega_m - \Omega_k$  plane for the  $\Lambda$ CDM (top) and DGP (bottom) models obtained with the SNe Ia gold sample plus the SDSS acoustic peak data and CMBR shift parameter (dashed lines). Also shown are the contours obtained assuming in addition a  $\mathcal{D}$  space topology with  $\gamma = 50^\circ \pm 6^\circ$ .

SDSS baryon oscillation data constrains basically  $\Omega_m$ , in agreement previous works [11,37–39]. Moreover, we see that the effect of including the topology constraint leads to a reduction of degeneracies, particularly relevant for the curvature parameter,  $\Omega_k$ .

Our results for the DT and Cardassian models are shown in Figs. 3 and 4 both with and without the topology constraint. The SNe + CMBR + BAO constraints lead to best-fit models that are, in both cases, closer to flat than the best-fit DGP model and closed spaces are preferred. Constraints on  $\Omega_m$  are similar for all models. The effect of topology is, for these models, again clearly important regarding the curvature parameter,  $\Omega_k$ , and does not affect significantly the remaining parameters.

In Fig. 5 we show how our results regarding the DGP and  $\Lambda$ CDM models depend on the angular radius of the circles,  $\gamma$ . This figure displays the lines of constant  $\gamma$  in the  $\Omega_k - \Omega_m$  plane for these models. We see that when the angular radius increases  $\Omega_k$  becomes more negative and that, for

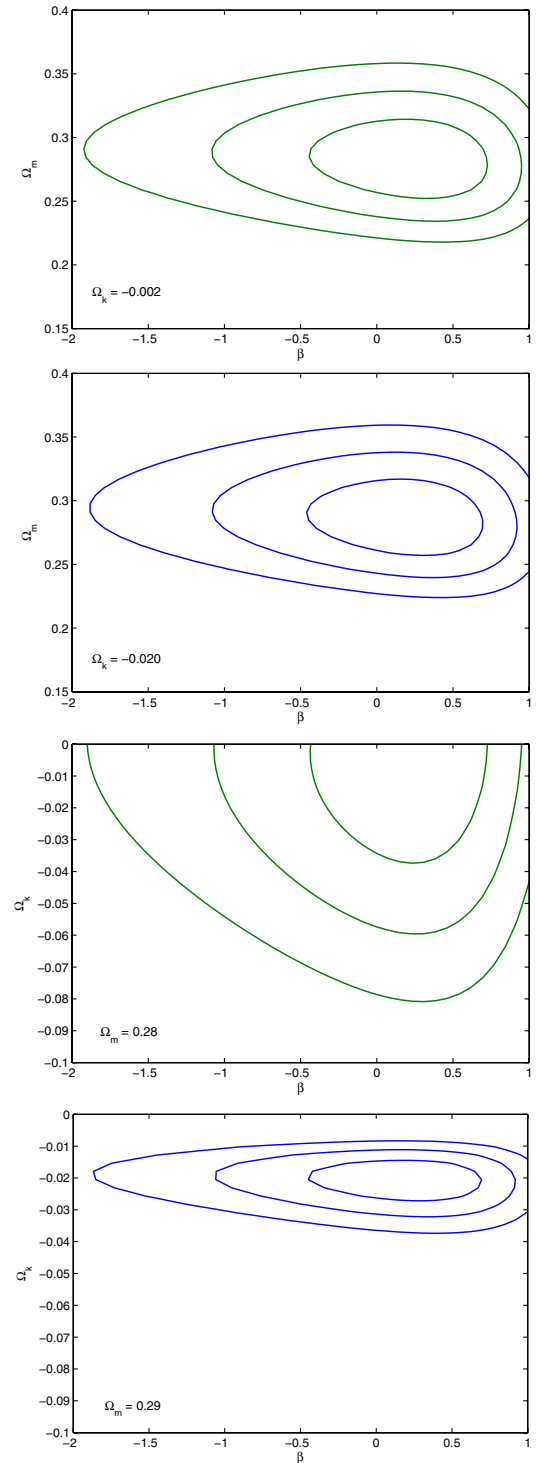


FIG. 3 (color online). Confidence contours (68.3%, 95.4% and 99.7%) for the DT model, in the  $\Omega_m - \beta$  and  $\Omega_k - \beta$  planes, obtained with the SN + SDSS + CMB data (first and third plots) and including also a  $\mathcal{D}$  space topology with  $\gamma = 50^\circ \pm 6^\circ$  (second and fourth plots).  $\Omega_k$  or  $\Omega_m$  are fixed at the value that minimizes the  $\chi^2$ .

any given value of the angular radius, the  $\Lambda$ CDM model prefers a less curved universe as compared with the DGP model. It is also clear that the bounds of topological origin

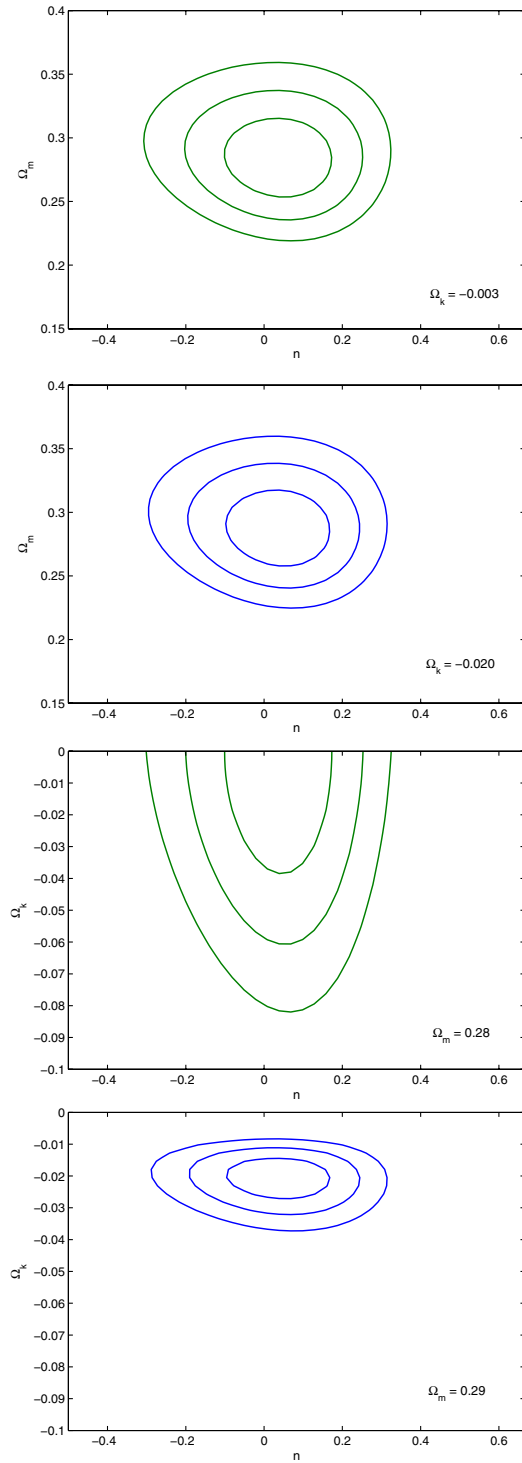


FIG. 4 (color online). Confidence contours (68.3%, 95.4% and 99.7%) for the Cardassian model, in the  $\Omega_m - n$  and  $\Omega_k - n$  planes, obtained with the SN + BAO + CMB data (first and third plots) and including also a  $\mathcal{D}$  space topology with  $\gamma = 50^\circ \pm 6^\circ$  (second and fourth plots).  $\Omega_k$  or  $\Omega_m$  are fixed at the value that minimizes the  $\chi^2$ .

on  $\Omega_k$  are expected to be very similar for both models, for any given angular radius in the interval  $60^\circ \lesssim \gamma \lesssim 10^\circ$ ; however, for  $\gamma \gtrsim 70^\circ$  the distinction between these bounds

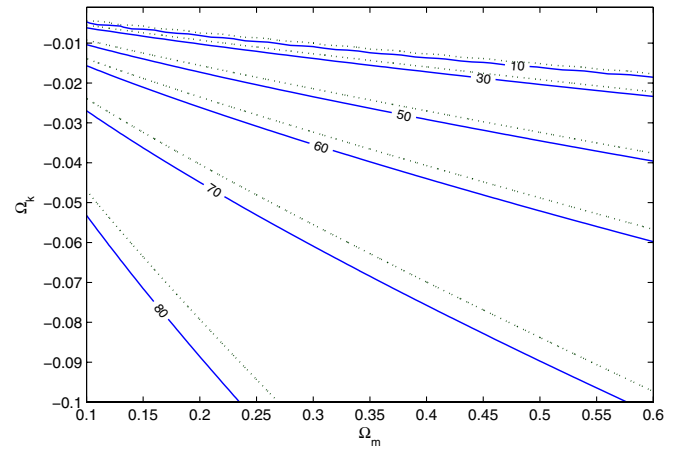


FIG. 5 (color online). Lines of constant angular radius,  $\gamma$ , in the  $\Omega_k - \Omega_m$  plane for the DGP (solid lines) and  $\Lambda$ CDM (dashed lines) models.

for the  $\Lambda$ CDM and DGP models becomes more important. Finally, this figure shows that the detection of circles predicted by the  $\mathcal{D}$  topology restricts substantially the range for  $\Omega_k$ , regardless of the angular radius  $\gamma$ . Clearly additional limits on this density parameter will arise for a specific value for  $\gamma$  and related uncertainty  $\delta\gamma$ . We find that, although the best fit for  $\Omega_k$  changes for different values of the angular radius,  $\gamma$ , this dependence is not very strong (see Fig. 5). For instance, if we assume a smaller value for  $\gamma$ , e.g.  $\gamma = 11^\circ \pm 1^\circ$ , as suggested in Ref. [45], the allowed regions will be shifted slightly towards values of  $\Omega_k$  closer to 0. On the other hand, changes in the uncertainty of the angular radius alter the area corresponding to the confidence regions.

## VI. CONCLUSIONS

We have analyzed observational constraints on models that account for the accelerated expansion of the universe that account for the accelerated expansion of the universe via long-range corrections to the Friedmann equation, namely, the Dvali-Gabadadze-Porrati braneworld model as well as the Dvali-Turner and Cardassian models. Using type Ia supernovae data together with the baryon acoustic peak in the large scale correlation function of the Sloan Digital Sky Survey of luminous red galaxies and the Cosmic Microwave Background Radiation shift parameter data, we find that significant constraints can be placed on the parameters of these models.

In general relativity, as well as in any metrical theory of gravitation of some generality and scope, a common approach to cosmological modeling commences with a space-time manifold endowed with a Lorentzian metric. The metrical approach to modeling the physical world has often led physicists to restrict their studies to the purely geometric features of space-time, either by ignoring the

role of spatial topology or by considering just the simply-connected topological alternatives. However, since the topological properties of a manifold are more fundamental than its metrical features, it is important to determine to what extent physical results related to a FLRW universe are constrained by the topology of its spatial section.

The so-called circles-in-the-sky method makes apparent that a nontrivial detectable topology of the spatial section of the universe is an observable attribute, and can be probed for any locally spatially homogeneous and isotropic space. By assuming the Poincaré dodecahedral space  $\mathcal{D}$  as the circles-in-the-sky detected topology of the spatial sections of the universe, we have reanalyzed the joint SNe + CMBR + BAO constraints on the above-mentioned mod-

els. The main outcome of our analysis is that the detection of a nontrivial spatial topology of the Universe through the circles-in-the-sky method would give rise to additional constraints on the curvature parameter for the models we have considered.

### ACKNOWLEDGMENTS

M. J. R. thanks CNPq for the grant under which this work was carried out, and is grateful to J. S. Alcaniz for useful discussions. The work of M. C. B. and O. B. was supported by Fundação para a Ciência e a Tecnologia (FCT, Portugal) under the grant No. POCI/FIS/56093/2004.

- 
- [1] G. R. Dvali, G. Gabadadze, and M. Porrati, *Phys. Lett. B* **485**, 208 (2000).
- [2] C. Deffayet, *Phys. Lett. B* **502**, 199 (2001).
- [3] G. Dvali and M. S. Turner, *astro-ph/0301510*.
- [4] K. Freese and M. Lewis, *Phys. Lett. B* **540**, 1 (2002).
- [5] V. Sahni and Y. Shtanov, *J. Cosmol. Astropart. Phys.* **11** (2003) 014.
- [6] A. G. Riess *et al.* (Supernova Search Team Collaboration), *Astrophys. J.* **607**, 665 (2004).
- [7] D. Eisenstein *et al.*, *Astrophys. J.* **633**, 560 (2005).
- [8] J. R. Bond, G. Efstathiou, and M. Tegmark, *Mon. Not. R. Astron. Soc.* **291**, L33 (1997); A. Melchiorri, L. Mersini-Houghton, C. J. Odman, and M. Trodden, *Phys. Rev. D* **68**, 043509 (2003).
- [9] K. Ichikawa and T. Takahashi, *Phys. Rev. D* **73**, 083526 (2006).
- [10] M. Amarzguioui, O. Elgaroy, D. F. Mota, and T. Multamaki, *astro-ph/0510519*.
- [11] R. Maartens and E. Majerotto, *astro-ph/0603353*.
- [12] M. C. Bento, O. Bertolami, N. M. C. Santos, and A. A. Sen, *Phys. Rev. D* **71**, 063501 (2005).
- [13] I. N. Bernshtein and V. F. Shvartsman, *Sov. Phys. JETP* **52**, 814 (1980).
- [14] M. Lachièze-Rey and J.-P. Luminet, *Phys. Rep.* **254**, 135 (1995); G. D. Starkman, *Classical Quantum Gravity* **15**, 2529 (1998); J. Levin, *Phys. Rep.* **365**, 251 (2002); M. J. Rebouças and G. I. Gomero, *Braz. J. Phys.* **34**, 1358 (2004); M. J. Rebouças, *astro-ph/0504365*.
- [15] R. Lehoucq, M. Lachièze-Rey, and J. P. Luminet, *Astron. Astrophys.* **313**, 339 (1996); B. F. Roukema, *Classical Quantum Gravity* **15**, 2645 (1998); R. Lehoucq, J. P. Luminet, and J. P. Uzan, *Astron. Astrophys.* **344**, 735 (1999); H. V. Fagundes and E. Gausmann, *Phys. Lett. A* **238**, 235 (1998); J. P. Uzan, R. Lehoucq, and J. P. Luminet, *Astron. Astrophys.* **351**, 766 (1999); G. I. Gomero, M. J. Rebouças, and A. F. F. Teixeira, *Int. J. Mod. Phys. D* **9**, 687 (2000); R. Lehoucq, J. P. Uzan, and J. P. Luminet, *Astron. Astrophys.* **363**, 1 (2000); G. I. Gomero, M. J. Rebouças, and A. F. F. Teixeira, *Phys. Lett. A* **275**, 355 (2000); *Classical Quantum Gravity* **18**, 1885 (2001); G. I. Gomero, A. F. F. Teixeira, M. J. Rebouças, and A. Bernui, *Int. J. Mod. Phys. D* **11**, 869 (2002); A. Marecki, B. Roukema, and S. Bajtlik, *Astron. Astrophys.* **435**, 427 (2005).
- [16] N. J. Cornish, D. Spergel, and G. D. Starkman, *Classical Quantum Gravity* **15**, 2657 (1998).
- [17] M. O. Calvão, G. I. Gomero, B. Mota, and M. J. Rebouças, *Classical Quantum Gravity* **22**, 1991 (2005).
- [18] D. N. Spergel *et al.*, *Astrophys. J. Suppl. Ser.* **148**, 175 (2003).
- [19] D. N. Spergel *et al.*, *astro-ph/0603449*.
- [20] R. Aurich, S. Lustig, and F. Steiner, *Classical Quantum Gravity* **22**, 2061 (2005).
- [21] R. Aurich, S. Lustig, and F. Steiner, *Classical Quantum Gravity* **22**, 3443 (2005).
- [22] J.-P. Luminet, J. Weeks, A. Riazuelo, R. Lehoucq, and J.-P. Uzan, *Nature (London)* **425**, 593 (2003).
- [23] M. J. Rebouças, J. S. Alcaniz, B. Mota, and M. Makler, *astro-ph/0511007*; M. J. Rebouças and J. S. Alcaniz, *astro-ph/0603206*; *Braz. J. Phys.* **35**, 1062 (2005).
- [24] A. Y. Kamenshchik, U. Moschella, and V. Pasquier, *Phys. Lett. B* **511**, 265 (2001).
- [25] N. Bilic, G. B. Tupper, and R. D. Viollier, *Phys. Lett. B* **535**, 17 (2002).
- [26] M. C. Bento, O. Bertolami, and A. A. Sen, *Phys. Rev. D* **66**, 043507 (2002); *Phys. Lett. B* **575**, 172 (2003); *Phys. Rev. D* **70**, 083519 (2004).
- [27] M. C. Bento, O. Bertolami, M. J. Rebouças, and P. T. Silva, *Phys. Rev. D* **73**, 043504 (2006).
- [28] C. Deffayet, G. Dvali, and G. Gabadadze, *Phys. Rev. D* **65**, 044023 (2002).
- [29] C. Deffayet, S. J. Landau, J. Raux, M. Zaldarriaga, and P. Astier, *Phys. Rev. D* **66**, 024019 (2002).
- [30] D. J. H. Chung and K. Freese, *Phys. Rev. D* **61**, 023511 (2000).
- [31] P. Gondolo and K. Freese, *Phys. Rev. D* **68**, 063509 (2003).
- [32] A. A. Sen and S. Sen, *Phys. Rev. D* **68**, 023513 (2003).

- [33] Y.G. Gong and C.K. Duan, *Mon. Not. R. Astron. Soc.* **352**, 847 (2004).
- [34] Z.H. Zhu, M.K. Fujimoto, and X.T. He, *Astrophys. J.* **603**, 365 (2004).
- [35] J.S. Alcaniz and N. Pires, *Phys. Rev. D* **70**, 047303 (2004).
- [36] O. Elgaroy and T. Multamaki, *Mon. Not. R. Astron. Soc.* **356**, 475 (2005).
- [37] M. Fairbairn and A. Goobar, astro-ph/0511029.
- [38] Zong-Kuan Guo, Zong-Hong Zhu, J.S. Alcaniz, and Yuan-Zhong Zhang, astro-ph/0603632.
- [39] U. Alam and V. Sahni, *Phys. Rev. D* **73**, 084024 (2006).
- [40] J.L. Tonry *et al.* (Supernova Search Team Collaboration), *Astrophys. J.* **594**, 1 (2003).
- [41] B.J. Barris *et al.*, *Astrophys. J.* **602**, 571 (2004).
- [42] J. Dick, L. Knox, and M. Chu, astro-ph/0603247.
- [43] G.I. Gomero, M.J. Rebouças, and R. Tavakol, *Classical Quantum Gravity* **18**, 4461 (2001); **18**, L145 (2001); *Int. J. Mod. Phys. A* **17**, 4261 (2002); J.R. Weeks, R. Lehoucq, and J.-P. Uzan, *Classical Quantum Gravity* **20**, 1529 (2003); J.R. Weeks, *Mod. Phys. Lett. A* **18**, 2099 (2003); G.I. Gomero and M.J. Rebouças, *Phys. Lett. A* **311**, 319 (2003); B. Mota, M.J. Rebouças, and R. Tavakol, *Classical Quantum Gravity* **20**, 4837 (2003).
- [44] N.J. Cornish, D.N. Spergel, G.D. Starkman, and E. Komatsu, *Phys. Rev. Lett.* **92**, 201302 (2004).
- [45] B.F. Roukema *et al.*, *Astron. Astrophys.* **423**, 821 (2004).
- [46] J. Gundermann, astro-ph/0503014.
- [47] R. Aurich, S. Lustig, and F. Steiner, astro-ph/0510847.
- [48] B. McInnes, *Phys. Lett. B* **593**, 10 (2004).
- [49] [http://cernlib.web.cern.ch/cernlib/download//2004\\_source/tar/minuit32\\_src.tar.gz](http://cernlib.web.cern.ch/cernlib/download//2004_source/tar/minuit32_src.tar.gz).